New Transmission Condition Accounting For Diffusion Anisotropy In Thin Layers Applied To Diffusion MRI

Fabien Caubet, Houssem Haddar, Jing-Rebecca Li, Dang Van Nguyen

NEW TRANSMISSION CONDITION ACCOUNTING FOR DIFFUSION ANISOTROPY IN THIN LAYERS APPLIED TO DIFFUSION MRI

FABIEN CAUBET*, HOUSSEM HADDAR†, JING-REBECCA LI‡, DANG VAN NGUYEN†

Abstract. The Bloch-Torrey Partial Differential Equation (PDE) can be used to model the diffusion Magnetic Resonance Imaging (dMRI) signal in biological tissue. In this paper, we derive an Anisotropic Diffusion Transmission Condition (ADTC) for the Bloch-Torrey PDE that accounts for anisotropic diffusion inside thin layers. Such diffusion occurs, for example, in the myelin sheath surrounding the axons of neurons. This ADTC can be interpreted as an asymptotic model of order two with respect to the layer thickness and accounts for water diffusion in the normal direction that is low compared to the tangential direction. We prove uniform stability of the asymptotic model with respect to the layer thickness and a mass conservation property. We demonstrate the quadratic accuracy of the ADTC by numerical tests and show that it gives a better approximation of the dMRI signal than a simple transmission condition that assumes isotropic diffusion in the layers.

Key words.

AMS subject classifications.

1. Introduction. Diffusion Magnetic Resonance Imaging (dMRI) gives a measure of the average distance travelled by water molecules in a medium and can give useful information on cellular structure and structural change when the medium is biological tissue. A large number of works have appeared in recent years that show that dMRI measurements can be correlated with various physiological or pathological conditions such as cell swelling, demyelinating disorders or the presence of tumors (see, for example, [17, 26, 20, 22, 19], and references therein). In particular, dMRI can be used to detect and quantify abnormalities in the myelin sheath surrounding the axons of neurons (see [11, 4, 7, 12]). The loss of or damage to the myelin sheath can be correlated with many diseases of brain function.

A commonly used mathematical model for water proton magnetization in tissue is the Bloch-Torrey (see [32]) Partial Differential Equation (PDE), where intrinsic diffusion tensors are defined in different cellular geometrical compartments. In this paper, we start with a three-compartment geometrical model: the three geometrical compartments are 1) the axons, 2) myelin sheath surrounding the axons, 3) the extra-cellular space. We want to approximate this original three-compartment model by a two-compartment geometrical model: the two geometrical compartments are 1) the axons and 2) the extra-cellular space. These two compartments will be linked via a transmission condition.

To obtain asymptotic two-compartment models, we rely on a methodology based on classical scaled asymptotic expansions for thin structures (see [28, 8, 10]) and on an appropriate scaling of tangential and normal diffusion inside the myelin layer. This methodology has been extensively used to model thin coatings (see e.g. [6, 14] and references therein), rough boundaries (see e.g. [1, 18] and references therein) and imperfectly conducting obstacles (see e.g. [15, 16] and references therein).

A simple and well-known transmission condition can be used when the diffusion inside the layer is isotropic. However, since the myelin sheath is composed of layers of lipids or proteins [29] (see Fig. 1 for an illustration), it is expected that the diffusion tensor in the myelin sheath will have a normal component that is much smaller than the tangential component (see discussion about diffusion inside the myelin sheath in [5, 21, 23]).

To account for low diffusion normal to the layer, we make the following choice for the diffusion inside the layer:

1. for the tangential direction, we use the same scaling as for diffusion in the axons and in the extra-cellular space;
2. for the normal direction, we use a scaling proportional to the layer thickness.

This choice leads to asymptotic transmission conditions. The first order approximation (in the layer thickness) leads to a transmission condition that has the same form as the classical trans-

*INSTITUT DE MATHÉMATIQUES DE TOULOUSE, UNIVERSITÉ DE TOULOUSE, F-31062 TOULOUSE CEDEX 9, FRANCE

†INRIA SACLAY, EQUIPE DÉFI, CMAP, ÉCOLE POLYTECHNIQUE, ROUTE DE SACLAY, 91128 PALAISEAU, FRANCE

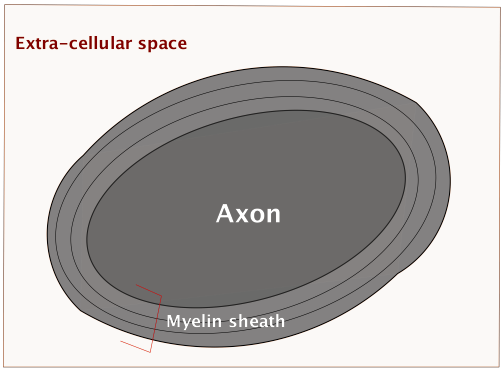

Figure 1: Illustration of the myelin sheath, composed of layers of lipids, surrounding the axon.

mission condition associated with isotropic layer diffusion. Anisotropy appears in the second order approximation and gives rise to our new Anisotropic Diffusion Transmission Condition (ADTC). This ADTC couples volumetric diffusion equations with surface diffusion equations. We note that the natural expression of the second order transmission condition does not exhibit uniform time stability with respect to the layer thickness, but this well-known phenomenon for higher order asymptotic models can be corrected by the use of Padé expansion, as in [13, 8], and our ADTC is corrected in this way. Thus, in its final form, our ADTC has a mass-conservation property, which is important for dMRI modeling.

We implemented a finite elements discretization of the new ADTC in two dimensions and conducted numerical tests that confirm second order accuracy with respect to layer thickness.

The ADTC that we propose here serves two purposes. From a numerical point of view, this approach simplifies the numerical solution of the dMRI model by removing the need to discretize the myelin sheath, a computational saving that may be significant in three dimensions when simulating arbitrarily oriented white matter fibers. Just as importantly, we hope that this reduction of the geometrical complexity of the model will aide in formulating a homogenized (macroscopic) model of the dMRI signal for white matter in the future. This will be the subject of future investigation.

The paper is organized as follows. We first explain the problem setting and describe the Bloch-Torrey equation in Section 2. Then, in Section 3, we detail the asymptotic method to obtain the new ADTC and prove uniform stability of the new model with respect to the layer thickness and a mass conservation property. Our numerical results are presented in Section 4. Conclusions are in Section 5.

2. Bloch-Torrey equation to model the diffusion MRI signal. A classic dMRI experiment consists of applying two pulsed gradient magnetic fields with a 180 degree spin reversal between the two pulses in order to encode the displacement of the water molecules between the two pulses [31]. The complex transverse water proton magnetization M can be modeled by the following Bloch-Torrey PDE [32]:

$$\frac{\partial M(\mathbf{x},t)}{\partial t} + i\mathbf{q}\cdot\mathbf{x} f(t) M(\mathbf{x},t) - \operatorname{div}\left(\overline{\boldsymbol{\sigma}}(\mathbf{x})\nabla M(\mathbf{x},t)\right) = 0, \tag{2.1}$$

where $i=\sqrt{-1}$, $\overline{\boldsymbol{\sigma}}(\mathbf{x})$ is the intrinsic diffusion tensor, $\mathbf{q}$ contains the amplitude and direction information of the applied diffusion-encoding magnetic field gradient multiplied by the gyro-magnetic ratio of the water proton, and f, where $\max_t f(t)=1$, is the normalized time profile of the diffusion-encoding magnetic field gradient sequence. The time profile of the classic Pulsed Gradient Spin Echo (PGSE) [31] sequence (simplified to include only the parameters relevant to diffusion, *i.e.*, the imaging gradients are ignored) is the following:

$$f(t) = \begin{cases} 1, & 0 < t \le \delta, \\ -1, & \Delta < t \le \Delta + \delta, \\ 0, & \text{elsewhere}, \end{cases} \tag{2.2}$$

where we made $f(t)$ negative in the second pulse to include the effect of the 180 degree spin reversal between the pulses. The time at which the signal is measured is called the echo time $TE > \delta + \Delta$.

The dMRI signal is the total magnetization:

$$S(\mathbf{q}) = \int M(\mathbf{x}, \delta + \Delta) \mathrm{d}\mathbf{x}, \tag{2.3}$$

where M is the solution of Eq. (2.1). The signal is usually plotted against a quantity called the $b-$value

$$b(\mathbf{q}) = \|\mathbf{q}\|^2 \delta^2 \left(\Delta - \frac{\delta}{3}\right), \tag{2.4}$$

because for a homogeneous domain, where $\overline{\boldsymbol{\sigma}}(\mathbf{x}) = \overline{\boldsymbol{\sigma}}$ is constant, the signal has the analytical expression:

$$S(\mathbf{q}) = \exp\left(-\left(\frac{\mathbf{q}^T \overline{\boldsymbol{\sigma}} \mathbf{q}}{\|\mathbf{q}\|^2}\right) b(\mathbf{q})\right), \tag{2.5}$$

where the quantity before the b-value is the diffusion coefficient in the direction of $\mathbf{q}$.

2.1. Geometrical compartments. A standard geometrical model of the brain white matter (for an early example, see [3]) divides the tissue into three compartments:

1. Ω_i^η is the axons (with associated intrinsic diffusion tensor $\overline{\boldsymbol{\sigma}}_i$);
2. Ω_e^η is the extra-cellular space (with associated intrinsic diffusion tensor $\overline{\boldsymbol{\sigma}}_e$);
3. Ω_m^η is the myelin sheath (with associated intrinsic diffusion tensor $\overline{\boldsymbol{\sigma}}_m$).

We denote by η the thickness of the layer (which is assumed to be constant) and by Γ a fictitious interface inside the myelin layer at equal distance from the two boundaries of the layer. We denote by Ω the domain formed by union of Ω_ℓ^η, $\ell = e, i, m$. We also introduce some notations as we consider the geometrical compartments when $\eta \to 0$: we denote the remaining two compartments by Ω_i and by Ω_e (see Figure 2). For the ease of notation, we restrict the diffusion tensor, $\overline{\boldsymbol{\sigma}}(\mathbf{x})$, for the tissue to be piece-wise constant:

$$\overline{\boldsymbol{\sigma}}(\mathbf{x}) = \begin{cases} \overline{\boldsymbol{\sigma}}_i, & \mathbf{x} \in \Omega_i^\eta, \\ \overline{\boldsymbol{\sigma}}_e, & \mathbf{x} \in \Omega_e^\eta, \\ \overline{\boldsymbol{\sigma}}_m, & \mathbf{x} \in \Omega_m^\eta. \end{cases} \tag{2.6}$$

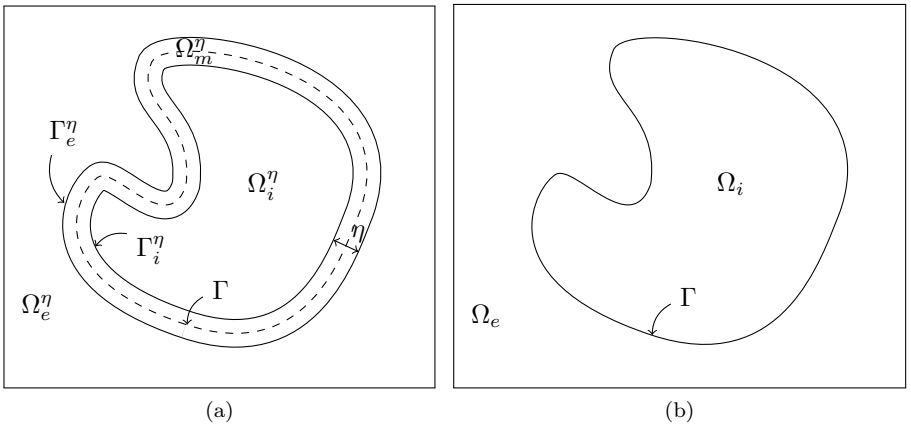

Figure 2: Notations for the three compartment model (left) and the two compartment model (right).

For the three compartment model, the natural continuity conditions (of the magnetization and the flux) on the compartment interfaces result is the following Interface Conditions (IC) on the

boundaries Γ_i^η and Γ_e^η of Ω_i^η and Ω_e^η:

$$\boxed{\text{IC on } \Gamma_e^\eta \text{ and } \Gamma_i^\eta \ : \ \begin{cases} [\overline{\boldsymbol{\sigma}} \nabla M \cdot \mathbf{n}] & = 0, \\ [M] & = 0, \end{cases}} \tag{2.7}$$

where $\mathbf{n}$ is the normal to Γ_i^η or Γ_i^η. The symbol $[\cdot]$ denotes the jump relative to the direction of $\mathbf{n}$.

Finally, the anisotropy inside the layer is assumed to be such that

$$\overline{\boldsymbol{\sigma}}_m \ : \ \begin{cases} \overline{\boldsymbol{\sigma}}_m \mathbf{n} & = \sigma_m^n \, \mathbf{n}, \\ \overline{\boldsymbol{\sigma}}_m \boldsymbol{\tau} & = \sigma_m^\tau \, \boldsymbol{\tau}, \end{cases} \tag{2.8}$$

where σ_m^n and σ_m^τ indicate respectively the transverse diffusion coefficient and tangential diffusion coefficient in the layer and $\boldsymbol{\tau}$ represents the unit tangential vector. The important assumption we make in this paper is that

$$\sigma_m^n \ll \sigma_m^\tau. \tag{2.9}$$

2.2. Classical asymptotic model for isotropic diffusion in layer. If the diffusion inside the layer is isotropic: $\sigma_m^n = \sigma_m^\tau$, it is well-known that the following asymptotic transmission condition, which we denote the *isotropic diffusion transmission condition* ("IDTC"), can be imposed on the interface Γ:

$$\boxed{\text{"IDTC" on } \Gamma \ : \ \begin{cases} [\overline{\boldsymbol{\sigma}} \nabla M \cdot \mathbf{n}] & = 0, \\ \overline{\boldsymbol{\sigma}} \nabla M \cdot \mathbf{n} & = \kappa_0 \, [M] \, , \ \kappa_0 \equiv \frac{\sigma_m}{\eta}. \end{cases}} \tag{2.10}$$

We recall that in addition to Eq. (2.10), the PDE (2.1) is assumed to hold on Ω^i and Ω^e. As we shall see, this type of transmission condition corresponds to a first order asymptotic model when the diffusion tensor inside the membrane scales like η. Our goal to improve this condition by taking into account the $O(1)$ tangential diffusion.

3. Formal derivation of transmission conditions . The methodology we shall adopt to derive transmission conditions is similar to the one in [6, 14, 15] and is based on a scaling of the layer with respect to its thickness η and an asymptotic expansion of the fields with respect to η. We shall restrict ourselves in this work to a formal obtention of these conditions (in the sense that no convergence proof will be established). However, this latter very technical step is usually valid (for linear problems) as long as the obtained model is proved to be uniformly stable with respect to the thickness. This is why we shall only discuss this last point. For technical details on convergence proofs (in other contexts) we refer the reader to [14, 15, 10]. The following formal technical details in space dimension 2 are largely inspired by [2] (see also [15] for space dimension 3).

3.1. Expression of the differential operators in curvilinear coordinates. We assume that Γ is a regular curve (at least C^2) and is the boundary of a simply connected domain Ω_i (independent from η). Notice that we can treat the case of multiply connected domains by treating separately each connected component. Then, the boundary Γ can be parametrized in terms of the curvilinear abscissa s as $s \mapsto \mathbf{x}_\Gamma(s)$, $s \in [0, L[$, with $|\mathrm{d}\mathbf{x}_\Gamma(s)/\mathrm{d}s| = 1$, where L is the length of Γ. We assume that this parametrization defines a clockwise orientation. Let $\mathbf{n}(s)$ be the unitary normal vector at $\mathbf{x}_\Gamma(s)$ directed to the exterior of Ω_i and set $\boldsymbol{\tau}(s) = \mathrm{d}\mathbf{x}_\Gamma(s)/\mathrm{d}s$ which is a unitary vector tangential to Γ at $\mathbf{x}_\Gamma(s)$. The curvature c can be defined by

$$c(s) := \boldsymbol{\tau}(s) \cdot \mathrm{d}\mathbf{n}(s)/\mathrm{d}s.$$

Let $\nu_0 := \inf_{0 \le s \le L} 1/|c(s)|$. Then, for $\eta < \nu_0$,

$$\forall \, \mathbf{x} \in \Omega_m^\eta, \exists ! (s, \nu) \in [0, L[\times] - \eta/2, \eta/2[, \ \mathbf{x} = \mathbf{x}_\Gamma(s) + \nu \, \mathbf{n}(s). \tag{3.1}$$

Notice that $\mathbf{x}_\Gamma$ is the orthogonal projection of $\mathbf{x}$ on Γ. The couple (s, ν) will be referred to as curvilinear (or parametric) coordinates of $\mathbf{x} \in \Omega_m^\eta$ (with respect to Γ). Let u be a function defined on Ω_m^η and let $\widetilde{u} : [0, L[\times] - \eta/2, \eta/2[$ be defined by

$$\widetilde{u}(s, \nu) := u(\mathbf{x}),$$

where $\mathbf{x}$ and (s,ν) satisfy Equation (3.1). Then, we have

$$\nabla u(\mathbf{x}) = \frac{1}{1+\nu c}\partial_s \widetilde{u}\,\boldsymbol{\tau} + \partial_\nu \widetilde{u}\,\mathbf{n} =: \frac{1}{1+\nu c}\nabla_\tau \widetilde{u} + \partial_\nu \widetilde{u}\,\mathbf{n} \tag{3.2}$$

and for a tensor $\overline{\boldsymbol{A}}$ such that $\overline{\boldsymbol{A}}\boldsymbol{\tau} = A^\tau\boldsymbol{\tau}$ and $\overline{\boldsymbol{A}}\mathbf{n} = A^n\mathbf{n}$, we have

$$\begin{aligned}\operatorname{div}\left(\overline{\boldsymbol{A}}\,\nabla u(\mathbf{x})\right) &= \frac{1}{1+\nu c}\partial_s\left(\frac{1}{1+\nu c}A^\tau\partial_s\,\widetilde{u}\right) + \frac{1}{1+\nu c}\partial_\nu\left((1+\nu c)A^n\partial_\nu\,\widetilde{u}\right)\\ &=: \frac{1}{1+\nu c}\operatorname{div}_\tau\left(\frac{1}{1+\nu c}A^\tau\nabla_\tau\widetilde{u}\right) + \frac{1}{1+\nu c}\partial_\nu\left((1+\nu c)A^n\partial_\nu\,\widetilde{u}\right).\end{aligned} \tag{3.3}$$

3.2. Scaling and formal asymptotic expansion. In order to take into account the relatively small values of the diffusion tensor along the normal coordinate we choose the scaling

$$\sigma_m^n = \kappa_0\,\eta \tag{3.4}$$

while we assume that $\overline{\boldsymbol{\sigma}}_e$, $\overline{\boldsymbol{\sigma}}_i$ and σ_m^τ are independent from η. We also scale the membrane Ω_m^η with respect to η and transform this domain into (the η independent domain) $\Gamma\times]-1/2,1/2[$ through the mapping $\mathbf{x}\mapsto(\mathbf{x}_\Gamma(s),\nu/\eta)$. Let us denote by M_ℓ the restriction of M to the domain Ω_ℓ for $\ell = e,i,m$. We then define $\widetilde{M}_m$ on $\Gamma\times]-1/2,1/2[\times[0,\infty)$ as

$$\widetilde{M}_m(\mathbf{x}_\Gamma,\xi,t) = M_m(\mathbf{x},t)$$

with $\xi := \frac{\nu}{\eta}$ and $\mathbf{x}$, $\mathbf{x}_\Gamma$ and ν satisfy (3.1). Since the time plays only the role of a parameter in the process of establishing membrane transmission condition, we shall omit indicating this variable in the notation. We first observe

$$\operatorname{div}\left(\overline{\boldsymbol{\sigma}}_m\nabla M_m\right) = \frac{1}{1+\eta\xi c}\operatorname{div}_\tau\left(\frac{1}{1+\eta\xi c}\sigma_m^\tau\nabla_\tau\widetilde{M}_m\right) + \frac{1}{\eta^2}\frac{1}{1+\eta\xi c}\partial_\xi\left((1+\eta\xi c)\eta\kappa_0\partial_\xi\widetilde{M}_m\right)$$

and also notice that

$$i\mathbf{q}\cdot\mathbf{x}\,f(t)M = i(\mathbf{q}\cdot\mathbf{x}_\Gamma + q^n\eta\xi)f(t)\widetilde{M}.$$

Assuming that $\widetilde{M}_m$ has the asymptotic expansion

$$\widetilde{M}_m(\mathbf{x}_\Gamma,\xi) = \sum_{k=0}^{\infty}\eta^k M_m^k(\mathbf{x}_\Gamma,\xi)$$

for some functions M_m^k defined on $\Gamma\times]-1/2,1/2[$, the Bloch-Torrey equation (multiplied by the factor $(1+\eta\xi)^3$) implies

$$\begin{aligned}\sum_{k=0}^{\infty}\eta^k\Big[&(1+\eta\xi)^3\partial_t M_m^k + (1+\eta\xi)^3 i(\mathbf{q}\cdot\mathbf{x}_\Gamma + q^n\eta\xi)f(t)M_m^k - (1+\eta\xi)\operatorname{div}_\tau\left(\sigma_m^\tau\nabla_\tau M_m^k\right)\\ &+ \eta\xi\sigma_m^\tau\nabla_\tau M_m^k\nabla_\tau c - \frac{\kappa_0}{\eta}(1+\eta\xi)^3\partial_{\xi\xi}^2 M_m^k - (1+\eta\xi)^2\kappa_0 c\partial_\xi M_m^k\Big] = 0.\end{aligned}$$

Then, by formal identification of powers of η, we obtain in particular for the first two terms

$$\kappa_0\partial_{\xi\xi}^2 M_m^0 = 0, \tag{3.5}$$

$$\kappa_0\partial_{\xi\xi}^2 M_m^1 = \partial_t M_m^0 + i\mathbf{q}\cdot\mathbf{x}_\Gamma f(t)M_m^0 - \operatorname{div}_\tau\left(\sigma_m^\tau\nabla_\tau M_m^0\right) - \kappa_0 c\partial_\xi M_m^0. \tag{3.6}$$

3.3. Derivation of ADTC. The expression of ADTC will be obtained from explicit expression of the solutions of (3.5) and (3.6) in terms of ξ and using the continuity conditions (2.7) that can be written in terms of $\widetilde{M}_m$ as

(3.7)
$$\begin{aligned} \widetilde{M}_m(\mathbf{x}_\Gamma,-\tfrac{1}{2}) &= M_i(\mathbf{x}_\Gamma-\tfrac{\eta}{2}\mathbf{n}), & \widetilde{M}_m(\mathbf{x}_\Gamma,\tfrac{1}{2}) &= M_e(\mathbf{x}_\Gamma+\tfrac{\eta}{2}\mathbf{n}),\\ \kappa_0\partial_\xi\widetilde{M}_m(\mathbf{x}_\Gamma,-\tfrac{1}{2}) &= \overline{\boldsymbol{\sigma}}_i\nabla M_i(\mathbf{x}_\Gamma-\tfrac{\eta}{2}\mathbf{n})\cdot\mathbf{n}, & \kappa_0\partial_\xi\widetilde{M}_m(\mathbf{x}_\Gamma,\tfrac{1}{2}) &= \overline{\boldsymbol{\sigma}}_e\nabla M_e(\mathbf{x}_\Gamma+\tfrac{\eta}{2}\mathbf{n})\cdot\mathbf{n}. \end{aligned}$$

In order to relate these boundary conditions to the asymptotic expansion of $\widetilde{M}_m$ we postulate that for $\ell = i, e$

$$M_\ell = \sum_{k=0}^{\infty} \eta^k M_\ell^k$$

where the functions M_ℓ^k are defined on Ω_ℓ and satisfy the Bloch-Torrey equation in Ω_ℓ. We shall distinguish two families of ATC according to the way we choose to match the three asymptotic expansions.

3.3.1. A first family of ADTC. A first family of ADTC is obtained by imposing the continuity conditions

$$M_m^k(\mathbf{x}_\Gamma,-\tfrac{1}{2}) = M_i^k(\mathbf{x}_\Gamma-\tfrac{\eta}{2}\mathbf{n}), \quad M_m^k(\mathbf{x}_\Gamma,\tfrac{1}{2}) = M_e^k(\mathbf{x}_\Gamma+\tfrac{\eta}{2}\mathbf{n}) \tag{3.8}$$

$$\kappa_0\partial_\xi M_m^k(\mathbf{x}_\Gamma,-\tfrac{1}{2}) = \overline{\boldsymbol{\sigma}}_i\nabla M_i^k(\mathbf{x}_\Gamma-\tfrac{\eta}{2}\mathbf{n})\cdot\mathbf{n}, \quad \kappa_0\partial_\xi M_m^k(\mathbf{x}_\Gamma,\tfrac{1}{2}) = \overline{\boldsymbol{\sigma}}_e\nabla M_e^k(\mathbf{x}_\Gamma+\tfrac{\eta}{2}\mathbf{n})\cdot\mathbf{n} \tag{3.9}$$

for all k, which is obtained from (3.7) by formal identification of powers of η. We remark that in this way the functions M_m^k depends also on η. Let us introduce the notation

$$\begin{aligned} \left\langle M^k\right\rangle_\eta(\mathbf{x}_\Gamma) &:= \frac{M_e^k(\mathbf{x}_\Gamma+\frac{\eta}{2}\mathbf{n}) + M_i^k(\mathbf{x}_\Gamma-\frac{\eta}{2})}{2}\\ \left[M^k\right]_\eta(\mathbf{x}_\Gamma) &:= M_e^k(\mathbf{x}_\Gamma+\tfrac{\eta}{2}) - M_i^k(\mathbf{x}_\Gamma-\tfrac{\eta}{2}\mathbf{n}) \end{aligned} \tag{3.10}$$

and similar definitions for $\left\langle\overline{\boldsymbol{\sigma}}\nabla M^k\cdot\mathbf{n}\right\rangle_\eta$ and $\left[\overline{\boldsymbol{\sigma}}\nabla M^k\cdot\mathbf{n}\right]_\eta$. We shall first express M_m^k (for $k=0,1$) in terms of $\left\langle M^k\right\rangle_\eta$ and $\left[M^k\right]_\eta$ by solving with respect to ξ Eqs. (3.5) and (3.6) using the two boundary conditions in (3.8). We then obtain an interface condition by using the two boundary conditions in (3.9). We can already remark that the obtained interface condition will not be a standard interface condition on Γ but will correspond to a condition that couples the boundary values at $\partial\Omega_e^\eta$ and $\partial\Omega_i^\eta$.

First order term.. From (3.5) and the boundary conditions in (3.8) one readily sees that

$$M_m^0 = \left\langle M^0\right\rangle_\eta + \xi\left[M^0\right]_\eta. \tag{3.11}$$

We then immediately get from (3.9)

$$\left[\overline{\boldsymbol{\sigma}}\nabla M^0\cdot\mathbf{n}\right]_\eta = 0 \text{ and } \left\langle\overline{\boldsymbol{\sigma}}\nabla M^0\cdot\mathbf{n}\right\rangle_\eta = \kappa_0\left[M^0\right]_\eta. \tag{3.12}$$

Second order term.. From (3.5) and (3.8) and using the expression (3.11) one gets

$$M_m^1(\mathbf{x}_\Gamma,\xi) = D_0(\mathbf{x}_\Gamma) + D_1(\mathbf{x}_\Gamma)\xi + D_2(\mathbf{x}_\Gamma)\xi^2 + D_3(\mathbf{x}_\Gamma)\xi^3 \tag{3.13}$$

where

$$\begin{aligned} D_0(\mathbf{x}_\Gamma) &= \left\langle M^1\right\rangle_\eta - \frac{1}{8\kappa_0}\left((\partial_t + i\mathbf{q}\cdot\mathbf{x}_\Gamma f(t))\left\langle M^0\right\rangle_\eta - \mathrm{div}_\tau\left(\sigma_m^\tau\nabla_\tau\left\langle M^0\right\rangle_\eta\right) - \kappa_0 c\left[M^0\right]_\eta\right)\\ D_1(\mathbf{x}_\Gamma) &= \left[M^1\right]_\eta - \frac{1}{24\kappa_0}\left((\partial_t + i\mathbf{q}\cdot\mathbf{x}_\Gamma f(t))\left[M^0\right]_\eta - \mathrm{div}_\tau\left(\sigma_m^\tau\nabla_\tau\left[M^0\right]_\eta\right)\right)\\ D_2(\mathbf{x}_\Gamma) &= \frac{1}{2\kappa_0}\left((\partial_t + i\mathbf{q}\cdot\mathbf{x}_\Gamma f(t))\left\langle M^0\right\rangle_\eta - \mathrm{div}_\tau\left(\sigma_m^\tau\nabla_\tau\left\langle M^0\right\rangle_\eta\right) - \kappa_0 c\left[M^0\right]_\eta\right)\\ D_3(\mathbf{x}_\Gamma) &= \frac{1}{6\kappa_0}\left((\partial_t + i\mathbf{q}\cdot\mathbf{x}_\Gamma f(t))\left[M^0\right]_\eta - \mathrm{div}_\tau\left(\sigma_m^\tau\nabla_\tau\left[M^0\right]_\eta\right)\right). \end{aligned}$$

We then conclude from (3.9)

$$
\begin{aligned}
\left[\overline{\boldsymbol{\sigma}}\nabla M^1\cdot\mathbf{n}\right]_\eta &= (\partial_t + i\mathbf{q}\cdot\mathbf{x}_\Gamma f(t))\left\langle M^0\right\rangle_\eta - \mathrm{div}_\tau\left(\sigma_m^\tau\nabla_\tau\left\langle M^0\right\rangle_\eta\right) - c\kappa_0\left[M^0\right]_\eta \\
\left\langle\overline{\boldsymbol{\sigma}}\nabla M^1\cdot\mathbf{n}\right\rangle_\eta &= \kappa_0\left[M^1\right]_\eta + \frac{1}{12}(\partial_t + i\mathbf{q}\cdot\mathbf{x}_\Gamma f(t))\left[M^0\right]_\eta - \frac{1}{12}\mathrm{div}_\tau\left(\sigma_m^\tau\nabla_\tau\left[M^0\right]_\eta\right).
\end{aligned}
\tag{3.14}
$$

A first ADTC of order two.. According to the conditions (3.12) and (3.14) and since $M_\ell = M_\ell^0 + \eta M_\ell^1 + \mathcal{O}(\eta^2)$ for $\ell = e, i$, we obtain the following interface approximate conditions

$$
\begin{aligned}
\left[\overline{\boldsymbol{\sigma}}\nabla M\cdot\mathbf{n}\right]_\eta &= \eta\left((\partial_t + i\mathbf{q}\cdot\mathbf{x}_\Gamma f(t))\left\langle M\right\rangle_\eta - \mathrm{div}_\tau\left(\sigma_m^\tau\nabla_\tau\left\langle M\right\rangle_\eta\right) - c\kappa_0\left[M\right]_\eta\right) + \mathcal{O}(\eta^2) \\
\left\langle\overline{\boldsymbol{\sigma}}\nabla M\cdot\mathbf{n}\right\rangle_\eta &= \kappa_0\left[M\right]_\eta + \frac{\eta}{12}\left((\partial_t + i\mathbf{q}\cdot\mathbf{x}_\Gamma f(t))\left[M\right]_\eta - \mathrm{div}_\tau\left(\sigma_m^\tau\nabla_\tau\left[M\right]_\eta\right)\right) + \mathcal{O}(\eta^2).
\end{aligned}
\tag{3.15}
$$

A membrane transmission condition of order 2 with respect to η is then obtained from (3.15) by dropping the $\mathcal{O}(\eta^2)$ terms. However, it turns out that the obtained expression does not lead to a diffusion problem that respect an energy identity similar to the original problem. This energy identity is important as it is supposed to provide uniform stability with respect to η. This stability is the main ingredient that guarantee the convergence rate at the consistency order (see e.g. [14, 15, 10] for similar problems).

In order to obtain an expression of ADTC that respects an uniform stability with respect to η, we shall replace the term $\eta\kappa_0\left[M\right]_\eta$ by $\eta\left\langle\overline{\boldsymbol{\sigma}}\nabla M\cdot\mathbf{n}\right\rangle_\eta$ in the first equation of (3.15) and add $\frac{\eta}{4}c\left[\overline{\boldsymbol{\sigma}}\nabla M\cdot\mathbf{n}\right]_\eta$ to the left hand side of the second equation (3.15). These substitutions, that have been suggested by the following energy proof, indeed do not change the formal $O(\eta^2)$ order of the reminders. We therefore propose as second order ADTC the following conditions

(3.16)

$$
\boxed{
\begin{cases}
\left[\overline{\boldsymbol{\sigma}}\nabla M\cdot\mathbf{n}\right]_\eta + \eta c\left\langle\overline{\boldsymbol{\sigma}}\nabla M\cdot\mathbf{n}\right\rangle_\eta = \eta\left((\partial_t + i\mathbf{q}\cdot\mathbf{x}_\Gamma f(t))\left\langle M\right\rangle_\eta - \mathrm{div}_\tau\left(\sigma_m^\tau\nabla_\tau\left\langle M\right\rangle_\eta\right)\right) \\
\left\langle\overline{\boldsymbol{\sigma}}\nabla M\cdot\mathbf{n}\right\rangle_\eta + \frac{\eta}{4}c\left[\overline{\boldsymbol{\sigma}}\nabla M\cdot\mathbf{n}\right]_\eta = \kappa_0\left[M\right]_\eta + \frac{\eta}{12}\left((\partial_t + i\mathbf{q}\cdot\mathbf{x}_\Gamma f(t))\left[M\right]_\eta - \mathrm{div}_\tau\left(\sigma_m^\tau\nabla_\tau\left[M\right]_\eta\right)\right).
\end{cases}
}
$$

Stability of ADTC (3.16). We shall outline the proof of an energy identity of the Bloch-Torrey equation

$$
\partial_t M(\mathbf{x},t) + i\,\mathbf{q}\cdot\mathbf{x}\,f(t)M(\mathbf{x},t) - \mathrm{div}\left(\sigma(\mathbf{x})\nabla M(\mathbf{x},t)\right) = 0 \qquad \text{in } \Omega_i^\eta\cup\Omega_e^\eta\times(0,T)
\tag{3.17}
$$

with the second order membrane transmission condition (3.16) on Γ. We only consider (for notation simplicity) the case where the diffusion in the axons and the extra-cellular space is isotropic, that is $\overline{\boldsymbol{\sigma}}_e = \sigma_e\mathrm{I}$ and $\overline{\boldsymbol{\sigma}}_i = \sigma_i\mathrm{I}$ (where I denotes the identity). Using the variational formulation with the conjugate $\overline{M}$ of M as test function, we obtain, denoting $\Omega^\eta := \Omega_i^\eta\cup\Omega_e^\eta$,

$$
\frac{1}{2}\frac{\mathrm{d}}{\mathrm{d}t}\int_{\Omega^\eta}|M|^2 + \int_{\Omega^\eta}\sigma\left|\nabla M\right|^2 + \int_{\Gamma_e^\eta}\mathfrak{Re}\left(\left(\sigma_e\nabla M^e\cdot\mathbf{n}\right)\overline{M^e}\right) - \int_{\Gamma_i^\eta}\mathfrak{Re}\left(\left(\sigma_i\nabla M^i\cdot\mathbf{n}\right)\overline{M^i}\right) = 0,
$$

where, $\mathfrak{Re}(z)$ denotes the real part of a complex number z. Using the changes of variables $\boldsymbol{y} = \mathbf{x}_\Gamma + \frac{\eta}{2}\mathbf{n}$ and $\boldsymbol{y} = \mathbf{x}_\Gamma - \frac{\eta}{2}\mathbf{n}$, we obtain the following equalities for a smooth enough function f (and small enough η)

$$
\int_{\partial\Omega_e^\eta} f\mathrm{d}s(\boldsymbol{y}) = \int_\Gamma\widetilde{f}\left(1+\frac{\eta}{2}c\right)\mathrm{d}s(\mathbf{x}) \text{ and } \int_{\partial\Omega_i^\eta} f\mathrm{d}s(\boldsymbol{y}) = \int_\Gamma\widetilde{f}\left(1-\frac{\eta}{2}c\right)\mathrm{d}s(\mathbf{x}).
$$

Hence, we obtain

$$
\begin{aligned}
\frac{1}{2}\frac{\mathrm{d}}{\mathrm{d}t}\int_{\Omega^\eta}|M|^2 + \int_{\Omega^\eta}\sigma\left|\nabla M\right|^2 + \int_\Gamma\mathfrak{Re}\left(\left(1+\frac{\eta}{2}c\right)\left(\sigma_e\nabla M^e\cdot\mathbf{n}\right)\overline{M^e}\right) \\
- \int_\Gamma\mathfrak{Re}\left(\left(1-\frac{\eta}{2}c\right)\left(\sigma_i\nabla M^i\cdot\mathbf{n}\right)\overline{M^i}\right) = 0.
\end{aligned}
\tag{3.18}
$$

Using the fact that

$$a^e b^e - a^i b^i = (a^e - a^i)\left(\frac{b^e + b^i}{2}\right) + (b^e - b^i)\left(\frac{a^e + a^i}{2}\right),$$

we obtain

$$\frac{1}{2}\frac{\mathrm{d}}{\mathrm{d}t}\int_{\Omega^\eta} |M|^2 + \int_{\Omega^\eta} \sigma\,|\nabla M|^2 + \int_\Gamma \mathfrak{Re}\left(\left([\sigma\nabla M\cdot\mathbf{n}]_\eta + \eta c\,\langle\sigma\nabla M\cdot\mathbf{n}\rangle_\eta\right)\langle\overline{M}\rangle_\eta\right) + \int_\Gamma \mathfrak{Re}\left(\left(\langle\sigma\nabla M\cdot\mathbf{n}\rangle_\eta + \frac{\eta}{4}c\,[\sigma\nabla M\cdot\mathbf{n}]_\eta\right)[\overline{M}]_\eta\right) = 0. \tag{3.19}$$

Using the ADTC (3.16), we end up with

$$\frac{1}{2}\frac{\mathrm{d}}{\mathrm{d}t}\int_{\Omega^\eta} |M|^2 + \int_{\Omega^\eta} \sigma\,|\nabla M|^2 + \kappa_0 \int_\Gamma \left|[M]_\eta\right|^2 + \eta\left(\frac{1}{2}\frac{\mathrm{d}}{\mathrm{d}t}\int_\Gamma \left|\langle M\rangle_\eta\right|^2 + \int_\Gamma \sigma_m^\tau \left|\langle\nabla_\tau M\rangle_\eta\right|^2\right) + \frac{\eta}{12}\left(\frac{1}{2}\frac{\mathrm{d}}{\mathrm{d}t}\int_\Gamma \left|[M]_\eta\right|^2 + \int_\Gamma \sigma_m^\tau \left|[\nabla_\tau M]_\eta\right|^2\right) = 0.$$

Let us finally notice that according to this energy estimate (and underlying variational formulation), the previous problem with the ADTC (3.16) is well-posed for H^1 initial data. Using the classical variational theory of Lions (see for instance [24, 25]) one can prove existence of solutions $M_\ell \in H^1(0,T;\mathrm{L}^2(\Omega_\ell^\eta)) \cap \mathrm{L}^2(0,T;\mathrm{H}^1(\Omega_\ell^\eta))$ (for $\ell = i, e$) such that $[M]_\eta$ and $\langle M\rangle_\eta$ are in $H^1(0,T;\mathrm{L}^2(\Gamma)) \cap \mathrm{L}^2(0,T;\mathrm{H}^1(\Gamma))$.

A conservation property for the ADTC (3.16). In dMRI, the measured signal corresponds to $\int_\Omega M$ and the application of a diffusion-encoding magnetic field gradient ($\mathbf{q} \neq \mathbf{0}$) induces attenuation of this quantity compared to the case $\mathbf{q} = 0$ (no attenuation). It is therefore important to check that our approximate model does not induce artificial attenuation when $\mathbf{q} = \mathbf{0}$.

When $\mathbf{q} = \mathbf{0}$, we easily obtain that

$$\int_{\Omega_e^\eta} \partial_t M_e + \int_{\Omega_i^\eta} \partial_t M_i + \int_{\partial\Omega_e^\eta} \overline{\boldsymbol{\sigma}}\nabla M_e\,\mathbf{n} - \int_{\partial\Omega_i^\eta} \overline{\boldsymbol{\sigma}}\nabla M_i\,\mathbf{n} = 0.$$

Using the changes of variables $\boldsymbol{y} = \mathbf{x}_\Gamma + \frac{\eta}{2}\,\mathbf{n}$ and $\boldsymbol{y} = \mathbf{x}_\Gamma - \frac{\eta}{2}\,\mathbf{n}$ in the boundary integrals, we obtain

$$\int_{\Omega_e^\eta} \partial_t M_e + \int_{\Omega_i^\eta} \partial_t M_i + \int_\Gamma [\overline{\boldsymbol{\sigma}}\nabla M\cdot\mathbf{n}]_\eta + \eta\int_\Gamma c\,\langle\overline{\boldsymbol{\sigma}}\nabla M\cdot\mathbf{n}\rangle_\eta = 0.$$

Therefore, using ADTC (3.16),

$$\int_{\Omega_e^\eta} \partial_t M_e + \int_{\Omega_i^\eta} \partial_t M_i + \int_\Gamma \eta\,\partial_t\langle M\rangle_\eta = 0.$$

In conclusion, we have the following mass conservation property, for all t,

$$\int_{\Omega_e^\eta\cup\Omega_i^\eta} M(\mathbf{x},t) + \eta\int_\Gamma \langle M(\mathbf{x},t)\rangle_\eta = \int_{\Omega_e^\eta\cup\Omega_i^\eta} M(\mathbf{x},0) + \eta\int_\Gamma \langle M(\mathbf{x},0)\rangle.$$

3.3.2. A second family of ADTC. We have to notice that the previous ADTC (3.16) have to be imposed numerically on each interface $\partial\Omega_m^\eta \cap \partial\Omega_e^\eta$ and $\partial\Omega_m^\eta \cap \partial\Omega_i^\eta$. However, in this case, we have numerically to manage a difficulty: the vertices on these interfaces would have to be aligned. To overcome this difficulty, we present here some additional computations based on Taylor expansion of M_e and M_i in order to obtain new ADTC imposed on the middle Γ of the membrane.

The second family of ADTC is obtained by using the previous postulate, for $\ell = i, e$,

$$M_\ell = \sum_{k=0}^{\infty} \eta^k M_\ell^k$$

and by using Taylor expansions of M_ℓ^k for all k, that is

$$M_\ell^k\left(\mathbf{x}_\Gamma+\frac{\eta}{2}\mathbf{n}\right)=M_\ell^k(\mathbf{x}_\Gamma)+\frac{\eta}{2}\nabla M_\ell^k(\mathbf{x}_\Gamma)\cdot\mathbf{n}+\frac{\eta^2}{4}\nabla^2 M_\ell^k(\mathbf{x}_\Gamma)\cdot\mathbf{n}\cdot\mathbf{n}+\mathcal{O}(\eta^3)$$
$$M_\ell^k\left(\mathbf{x}_\Gamma-\frac{\eta}{2}\mathbf{n}\right)=M_\ell^k(\mathbf{x}_\Gamma)-\frac{\eta}{2}\nabla M_\ell^k(\mathbf{x}_\Gamma)\cdot\mathbf{n}+\frac{\eta^2}{4}\nabla^2 M_\ell^k(\mathbf{x}_\Gamma)\cdot\mathbf{n}\cdot\mathbf{n}+\mathcal{O}(\eta^3).$$

Hence, using the continuity conditions (3.7) and a formal identification of powers of η, we obtain (for $k=0,1$):

$$\begin{aligned}
M_m^0(\mathbf{x}_\Gamma,-\frac{1}{2}) &= M_i^0(\mathbf{x}_\Gamma)\\
M_m^0(\mathbf{x}_\Gamma,\frac{1}{2}) &= M_e^0(\mathbf{x}_\Gamma)\\
M_m^1(\mathbf{x}_\Gamma,-\frac{1}{2}) &= M_i^1(\mathbf{x}_\Gamma)-\frac{1}{2}\nabla M_i^0(\mathbf{x}_\Gamma)\cdot\mathbf{n}\\
M_m^1(\mathbf{x}_\Gamma,\frac{1}{2}) &= M_e^1(\mathbf{x}_\Gamma)+\frac{1}{2}\nabla M_e^0(\mathbf{x}_\Gamma)\cdot\mathbf{n}
\end{aligned}\tag{3.20}$$

and

$$\begin{aligned}
\kappa_0\partial_\xi M_m^0(\mathbf{x}_\Gamma-\frac{1}{2}) &= \overline{\boldsymbol{\sigma}}_i\nabla M_i^0(\mathbf{x}_\Gamma)\cdot\mathbf{n}\\
\kappa_0\partial_\xi M_m^0(\mathbf{x}_\Gamma+\frac{1}{2}) &= \overline{\boldsymbol{\sigma}}_e\nabla M_e^0(\mathbf{x}_\Gamma)\cdot\mathbf{n}\\
\kappa_0\partial_\xi M_m^1(\mathbf{x}_\Gamma-\frac{1}{2}) &= \overline{\boldsymbol{\sigma}}_i\nabla M_i^1(\mathbf{x}_\Gamma)\cdot\mathbf{n}-\frac{1}{2}\overline{\boldsymbol{\sigma}}_i\nabla^2 M_-^0(\mathbf{x}_\Gamma)\cdot\mathbf{n}\cdot\mathbf{n}\\
\kappa_0\partial_\xi M_m^1(\mathbf{x}_\Gamma+\frac{1}{2}) &= \overline{\boldsymbol{\sigma}}_e\nabla M_e^1(\mathbf{x}_\Gamma)\cdot\mathbf{n}+\frac{1}{2}\overline{\boldsymbol{\sigma}}_e\nabla^2 M_+^0(\mathbf{x}_\Gamma)\cdot\mathbf{n}\cdot\mathbf{n}.
\end{aligned}\tag{3.21}$$

We recall the notations

$$\begin{aligned}
\left\langle M^k\right\rangle(\mathbf{x}_\Gamma) &:= \frac{M_e^k(\mathbf{x}_\Gamma)+M_i^k(\mathbf{x}_\Gamma)}{2}\\
\left[M^k\right](\mathbf{x}_\Gamma) &:= M_e^k(\mathbf{x}_\Gamma)-M_i^k(\mathbf{x}_\Gamma).
\end{aligned}\tag{3.22}$$

We then follow the same strategy than in the previous subsection: we first express M_m^k (for $k=0,1$) in terms of $\left\langle M^k\right\rangle$ and $\left[M^k\right]$ by solving with respect to ξ Eqs. (3.5) and (3.6) using the previous boundary conditions in (3.20). We then obtain an interface condition by using the boundary conditions (3.21).

First order term. From (3.5) and the boundary conditions in (3.20) one finds exactly the same conditions as in Section 3.3.1:

$$M_m^0=\left\langle M^0\right\rangle+\xi\left[M^0\right]\tag{3.23}$$

and, from (3.21),

$$\left[\overline{\boldsymbol{\sigma}}\nabla M^0\cdot\mathbf{n}\right]=0 \text{ and } \left\langle\overline{\boldsymbol{\sigma}}\nabla M^0\cdot\mathbf{n}\right\rangle=\kappa_0\left[M^0\right].\tag{3.24}$$

Second order term. Proceeding as in Section 3.3.1, one gets from (3.5) and (3.20) and using the expression (3.23),

$$M_m^1(\mathbf{x}_\Gamma,\xi)=F_0(\mathbf{x}_\Gamma)+F_1(\mathbf{x}_\Gamma)\xi+F_2(\mathbf{x}_\Gamma)\xi^2+F_3(\mathbf{x}_\Gamma)\xi^3\tag{3.25}$$

where

$$F_0(\mathbf{x}_\Gamma)=\left\langle M^1\right\rangle+\frac{1}{4}\left[\nabla M^0\cdot\mathbf{n}\right]-\frac{1}{8\kappa_0}\left(\left(\partial_t+i\mathbf{q}\cdot\mathbf{x}_\Gamma f(t)\right)\left\langle M^0\right\rangle-\mathrm{div}_\tau\left(\sigma_m^\tau\nabla_\tau\left\langle M^0\right\rangle\right)-\kappa_0 c\left[M^0\right]\right)$$
$$F_1(\mathbf{x}_\Gamma)=\left[M^1\right]+\left\langle\nabla M^0\cdot\mathbf{n}\right\rangle-\frac{1}{24\kappa_0}\left(\left(\partial_t+i\mathbf{q}\cdot\mathbf{x}_\Gamma f(t)\right)\left[M^0\right]-\mathrm{div}_\tau\left(\sigma_m^\tau\nabla_\tau\left[M^0\right]\right)\right)$$
$$F_2(\mathbf{x}_\Gamma)=\frac{1}{2\kappa_0}\left(\left(\partial_t+i\mathbf{q}\cdot\mathbf{x}_\Gamma f(t)\right)\left\langle M^0\right\rangle-\mathrm{div}_\tau\left(\sigma_m^\tau\nabla_\tau\left\langle M^0\right\rangle\right)-\kappa_0 c\left[M^0\right]\right)$$
$$F_3(\mathbf{x}_\Gamma)=\frac{1}{6\kappa_0}\left(\left(\partial_t+i\mathbf{q}\cdot\mathbf{x}_\Gamma f(t)\right)\left[M^0\right]-\mathrm{div}_\tau\left(\sigma_m^\tau\nabla_\tau\left[M^0\right]\right)\right).$$

One can notice that $F_2 = D_2$ and $F_3 = D_3$, where D_2 and D_3 are defined in (3.13).

We then conclude from (3.21)

(3.26)
$$\begin{aligned}
&\left[\overline{\boldsymbol{\sigma}}\nabla M^1\cdot\mathbf{n}\right] + \left\langle\overline{\boldsymbol{\sigma}}\nabla^2 M^0\cdot\mathbf{n}\cdot\mathbf{n}\right\rangle \\
&\qquad = \quad (\partial_t + i\mathbf{q}\cdot\mathbf{x}_\Gamma f(t))\left\langle M^0\right\rangle - \mathrm{div}_\tau\left(\sigma_m^\tau\nabla_\tau\left\langle M^0\right\rangle\right) - c\kappa_0\left[M^0\right] \\
&\left\langle\overline{\boldsymbol{\sigma}}\nabla M^1\cdot\mathbf{n}\right\rangle + \frac{1}{4}\left[\overline{\boldsymbol{\sigma}}\nabla^2 M^0\cdot\mathbf{n}\cdot\mathbf{n}\right] \\
&\qquad = \quad \kappa_0\left[M^1\right] + \kappa_0\left\langle\nabla M^0\cdot\mathbf{n}\right\rangle + \frac{1}{12}\Big((\partial_t + i\mathbf{q}\cdot\mathbf{x}_\Gamma f(t))\left[M^0\right] - \mathrm{div}_\tau\left(\sigma_m^\tau\nabla_\tau\left[M^0\right]\right)\Big).
\end{aligned}$$

Moreover, we have on Γ, for $\ell = i, e$,

$$\overline{\boldsymbol{\sigma}}_\ell\nabla^2 M_\ell^0\cdot\mathbf{n}\cdot\mathbf{n} = \partial_t M_\ell^0 + i\mathbf{q}\cdot\mathbf{x}_\Gamma f(t) M_\ell^0 - \mathrm{div}_\tau\left(\overline{\boldsymbol{\sigma}}_\ell\nabla_\tau M_\ell^0\right) - c\,\overline{\boldsymbol{\sigma}}_\ell\nabla M_\ell^0\cdot\mathbf{n}.$$

Hence, using (3.24), we obtain

$$\begin{aligned}
\left[\overline{\boldsymbol{\sigma}}\nabla M^1\cdot\mathbf{n}\right] &= \mathrm{div}_\tau\left(\left\langle(\overline{\boldsymbol{\sigma}} - \sigma_m^\tau\mathrm{I})\nabla_\tau M^0\right\rangle\right) \\
\left\langle\overline{\boldsymbol{\sigma}}\nabla M^1\cdot\mathbf{n}\right\rangle &= \kappa_0\left[M^1\right] + \kappa_0\left\langle\nabla M^0\cdot\mathbf{n}\right\rangle - \frac{1}{6}\Bigg((\partial_t + i\mathbf{q}\cdot\mathbf{x}_\Gamma f(t))\left[M^0\right] \\
&\qquad + \frac{1}{2}\mathrm{div}_\tau\left(\sigma_m^\tau\nabla_\tau\left[M^0\right]\right)\Bigg) + \frac{1}{4}\mathrm{div}_\tau\left(\left[\overline{\boldsymbol{\sigma}}\nabla_\tau M^0\right]\right).
\end{aligned}$$

In order to obtain an energy identity (see below), we rewrite these conditions as

(3.27)
$$\begin{aligned}
\left[\overline{\boldsymbol{\sigma}}\nabla M^1\cdot\mathbf{n}\right] &= \mathrm{div}_\tau\left(\left\langle(\overline{\boldsymbol{\sigma}} - \sigma_m^\tau\mathrm{I})\nabla_\tau M^0\right\rangle\right) \\
\left\langle\overline{\boldsymbol{\sigma}}\nabla M^1\cdot\mathbf{n}\right\rangle &= \kappa_0\left[M^1\right] + \kappa_0\left\langle\nabla M^0\cdot\mathbf{n}\right\rangle - \frac{1}{6}\Bigg((\partial_t + i\mathbf{q}\cdot\mathbf{x}_\Gamma f(t))\left[M^0\right] \\
&\qquad - \mathrm{div}_\tau\left(\sigma_m^\tau\nabla_\tau\left[M^0\right]\right)\Bigg) + \frac{1}{4}\mathrm{div}_\tau\left(\left[(\overline{\boldsymbol{\sigma}} - \sigma_m^\tau\mathrm{I})\nabla_\tau M^0\right]\right).
\end{aligned}$$

A second ADTC of order two. According to the conditions (3.24) and (3.27) and since $M_\ell = M_\ell^0 + \eta M_\ell^1 + \mathcal{O}(\eta^2)$ for $\ell = e, i$, we obtain the following interface approximate conditions

(3.28)
$$\begin{aligned}
[\overline{\boldsymbol{\sigma}}\nabla M\cdot\mathbf{n}] &= \eta\,\mathrm{div}_\tau\left(\left\langle(\overline{\boldsymbol{\sigma}} - \sigma_m^\tau\mathrm{I})\nabla_\tau M\right\rangle\right) + \mathcal{O}(\eta^2) \\
\left\langle\overline{\boldsymbol{\sigma}}\nabla M\cdot\mathbf{n}\right\rangle &= \kappa_0\left[M\right] - \frac{\eta}{6}P\left([M]\right) + \frac{\eta}{4}\mathrm{div}_\tau\left([(\overline{\boldsymbol{\sigma}} - \sigma_m^\tau\mathrm{I})\nabla_\tau M]\right) + \mathcal{O}(\eta^2),
\end{aligned}$$

where

$$P\left([M]\right) := (\partial_t + i\mathbf{q}\cdot\mathbf{x}_\Gamma f(t))\left[M\right] - \mathrm{div}_\tau\left(\sigma_m^\tau\nabla_\tau\left[M\right]\right).$$

The ADTC resulting from (3.28) turns out to be unconditionally unstable (similarly to what observed in [14, 10] for a different prblem). In order to obtain a stable problem we shall replace the operator $\kappa_0\left[M\right] - \frac{\eta}{6}P$ by a Padé approximation up to $O(\eta^2)$ terms (which is compatible with the ADTC order). More precisely, we introduce an auxilary unknown Ψ on Γ that satisfies

$$\left(1 + \frac{\eta}{6\kappa_0}P\right)\Psi = [M]$$

in such a way that

$$\left\langle\overline{\boldsymbol{\sigma}}\nabla M\cdot\mathbf{n}\right\rangle = \kappa_0\Psi + \frac{\eta}{4}\mathrm{div}_\tau\left([(\overline{\boldsymbol{\sigma}} - \sigma_m^\tau\mathrm{I})\nabla_\tau M]\right) - \frac{1}{2}\frac{\eta^2}{6^2\kappa_0^2}P\left(P\left(\Psi\right)\right) + \mathcal{O}(\eta^2).$$

By neglecting all $\mathcal{O}(\eta^2)$ terms we end up with a second order membrane transmission condition on Γ in the following form:

(3.29)
$$\boxed{\begin{cases}
[\overline{\boldsymbol{\sigma}}\nabla M\cdot\mathbf{n}] &= \eta\,\mathrm{div}_\tau\left(\left\langle(\overline{\boldsymbol{\sigma}} - \sigma_m^\tau\mathrm{I})\nabla_\tau M\right\rangle\right), \\
\left\langle\overline{\boldsymbol{\sigma}}\nabla M\cdot\mathbf{n}\right\rangle &= \kappa_0\Psi + \dfrac{\eta}{4}\mathrm{div}_\tau\left([(\overline{\boldsymbol{\sigma}} - \sigma_m^\tau\mathrm{I})\nabla_\tau M]\right),
\end{cases}}$$

where

$$\boxed{\begin{cases} \left(1+\frac{\eta}{6\kappa_0}P\right)\Psi &=& [M]\,, \\ \Psi &=& 0 \quad \text{at } t=0. \end{cases}} \tag{3.30}$$

Remark 1. *We can note that, in the specific case where* $\overline{\boldsymbol{\sigma}}_e = \overline{\boldsymbol{\sigma}}_i = \sigma_m^\tau \mathrm{I}$*, the second order ADTC has the simple form*

$$\begin{aligned} [\overline{\boldsymbol{\sigma}}\nabla M\cdot\mathbf{n}] &= 0 \\ \langle\overline{\boldsymbol{\sigma}}\nabla M\cdot\mathbf{n}\rangle &= \kappa_0\Psi. \end{aligned} \tag{3.31}$$

where Ψ *satisfies* (3.30).

Stability of ADTC (3.29–3.30). Here again, for notation simplicity, we assume that $\overline{\boldsymbol{\sigma}}_e = \sigma_e \mathrm{I}$ and $\overline{\boldsymbol{\sigma}}_i = \sigma_i \mathrm{I}$ in this paragraph. Then, proceeding similarly to Section 3.3.1 (notice that here the volumetric equations are valid in $\Omega_i \cup \Omega_e$), we obtain

$$\begin{aligned} \frac{1}{2}\frac{\mathrm{d}}{\mathrm{d}t}\int_\Omega |M|^2 + \int_\Omega \sigma\,|\nabla M|^2 - \eta\int_\Gamma \mathfrak{Re}\left(\langle(\sigma-\sigma_m^\tau)\nabla_\tau M\rangle\cdot\langle\nabla_\tau\overline{M}\rangle\right) + \kappa_0\int_\Gamma |\Psi|^2 \\ + \frac{\eta}{6}\frac{1}{2}\frac{\mathrm{d}}{\mathrm{d}t}\int_\Gamma |\Psi|^2 + \frac{\eta}{6}\int_\Gamma \sigma_m^\tau\,|\nabla_\tau\Psi|^2 - \frac{\eta}{4}\int_\Gamma \mathfrak{Re}\left([(\sigma-\sigma_m^\tau)\nabla_\tau M]\cdot[\nabla_\tau\overline{M}]\right) = 0. \end{aligned}$$

Hence, using the fact that

$$\begin{aligned} a^e b^e + a^i b^i &= 2\left(\frac{a^e+a^i}{2}\right)\left(\frac{b^e+b^i}{2}\right) + \frac{1}{2}(a^e-a^i)(b^e-b^i) \\ a^e b^e - a^i b^i &= (a^e-a^i)\left(\frac{b^e+b^i}{2}\right) + \left(\frac{a^e+a^i}{2}\right)(b^e-b^i), \end{aligned}$$

we have

$$\begin{aligned} \int_\Gamma \langle(\sigma-\sigma_m^\tau)\nabla_\tau M\rangle\cdot\langle\nabla_\tau\overline{M}\rangle &= \int_\Gamma \langle\sigma-\sigma_m^\tau\rangle\,|\langle\nabla_\tau M\rangle|^2 + \frac{1}{4}\int_\Gamma [\sigma-\sigma_m^\tau]\,[\nabla_\tau M]\cdot\langle\nabla_\tau\overline{M}\rangle \\ \int_\Gamma [(\sigma-\sigma_m^\tau)\nabla_\tau M]\cdot[\nabla_\tau\overline{M}] &= \int_\Gamma [\sigma-\sigma_m^\tau]\,\langle\nabla_\tau M\rangle\cdot[\nabla_\tau\overline{M}] + \int_\Gamma \langle\sigma-\sigma_m^\tau\rangle\,|[\nabla_\tau M]|^2 \end{aligned}$$

and then, we obtain

$$\begin{aligned} \frac{1}{2}\frac{\mathrm{d}}{\mathrm{d}t}\int_\Omega |M|^2 + \int_\Omega \sigma\,|\nabla M|^2 + \kappa_0\int_\Gamma |\Psi|^2 + \frac{\eta}{12}\frac{\mathrm{d}}{\mathrm{d}t}\int_\Gamma |\Psi|^2 + \frac{\eta}{6}\int_\Gamma \sigma_m^\tau\,|\nabla_\tau\Psi|^2 \\ + \eta\int_\Gamma \langle\sigma_m^\tau-\sigma\rangle\,|\langle\nabla_\tau M\rangle|^2 + \frac{\eta}{4}\int_\Gamma \langle\sigma_m^\tau-\sigma\rangle\,|[\nabla_\tau M]|^2 - \frac{\eta}{2}\int_\Gamma \mathfrak{Re}\left([\sigma]\,[\nabla_\tau M]\cdot\langle\nabla_\tau\overline{M}\rangle\right) = 0. \end{aligned}$$

Therefore, the stability is guaranteed as soon as the positivity of the terms in the second line of the above identity is ensured. This holds if

$$\langle\sigma_m^\tau-\sigma\rangle \geq 0 \text{ and } 4\,\langle\sigma_m^\tau-\sigma\rangle^2 - [\sigma]^2 \geq 0.$$

Remark 2. *We can notice that the stability is ensured if* $\sigma_e = \sigma_i = \sigma_m^\tau$*. We also notice that in the case* $\sigma_e = \sigma_i = \sigma$ *the stability requires* $\sigma_m^\tau \geq \sigma$*, which is compatible with the observations in [10] for the case of the wave equation.* We finally notice that when the stability holds, it is also easy to prove well posedness of the Bloch-torrey equations coupled with ADTC (3.29–3.30). With L^2 initial data for M_ℓ, $\ell = i, e$, one can prove the existence and uniqueness of solutions (using the classical variational theory of Lions (see for instance [24, 25])) $M_\ell \in H^1(0,T;\mathrm{L}^2(\Omega_\ell))\cap\mathrm{L}^2(0,T;\mathrm{H}^1(\Omega_\ell))$ and $\Psi \in H^1(0,T;\mathrm{L}^2(\Gamma))\cap\mathrm{L}^2(0,T;\mathrm{H}^1(\Gamma))$.

A conservation property for the ADTC (3.29–3.30). Let us check again that our approximate model does not induce artificial attenuation in the case $\mathbf{q} = \mathbf{0}$. Indeed if $\mathbf{q} = \mathbf{0}$,

$$\int_{\Omega_e} \partial_t M_e + \int_{\Omega_i} \partial_t M_i + \int_{\partial\Omega_e} \overline{\boldsymbol{\sigma}} \nabla M_e \cdot \mathbf{n} - \int_{\partial\Omega_i} \overline{\boldsymbol{\sigma}} \nabla M_i \cdot \mathbf{n} = 0.$$

According to the new ADTC (3.29–3.30), $[\overline{\boldsymbol{\sigma}} \nabla M \cdot \mathbf{n}] = \eta \, \mathrm{div}_\tau \left(\langle (\overline{\boldsymbol{\sigma}} - \sigma_m^\tau \mathrm{I}) \nabla_\tau M \rangle \right)$. We therefore immediately obtain by integration by parts on Γ

$$\int_{\Omega_e} \partial_t M_e + \int_{\Omega_i} \partial_t M_i = 0.$$

In conclusion,

$$\int_{\Omega_e \cup \Omega_i} M(\mathbf{x}, t) = \int_{\Omega_e \cup \Omega_i} M(\mathbf{x}, 0) \text{ for all } t > 0.$$

4. Numerical validation. We numerically solve three models of the dMRI signal in the presence of thin layers:

1. the original three-compartment model where Ω_i^η, Ω_m^η, Ω_e^η are linked by the interface conditions on Γ_i^η and Γ_e^η (see Eq. (2.7));
2. the classical asymptotic two-compartment model where Ω^e and Ω^i are linked by the isotropic diffusion transmission condition ("IDTC", see Eq. (2.10));
3. the new asymptotic two-compartment model where Ω^e and Ω^i are linked by the anisotropic diffusion transmission condition ("ADTC", see Eqs. (3.29 and 3.30)).

We compute the dMRI signal associated with each of the three models. We compare the accuracy of the two asymptotic models in approximating the dMRI signal of the original three-compartment model as $\eta \to 0$. We note here that to implement the "ADTC", at each time step, we solve Eq. (3.30) on the interface (in $d-1$ dimension) with given jump $[M]$ to obtain Ψ. Then, we solve the Bloch-Torrey equation (2.1) with the Neumann boundary conditions (3.29) (in d dimensions).

The simulations were performed in $d = 2$ dimensions and the numerical method proposed in [27] was used and modified to solve the PDEs, where linear finite elements are coupled with the explicit Runge-Kutta Chebyshev (RKC) [33, 30] time stepping. The numerical code is implemented on FEniCS C++ platform and we used Salome 6.6.0 to generate finite element meshes. All simulations were performed on a Lenovo workstation (Intel(R) Xeon(R) CPU X3430@2.40GB), running the program as a serial code on Linux Ubuntu 10.04 LTS.

The computational domain C is chosen to be $[-5\mu\mathrm{m}, 5\mu\mathrm{m}]^2$, containing an irregularly shaped axon. The thickness of the myelin sheath, η, is varied between 0.1μm and 1.5μm. We set the maximum finite element diameter to 0.05μm. The absolute tolerance 10^{-12} and relative tolerance 10^{-10} were set for the iterative linear solver GMRES, and the absolute and relative tolerance used for the RKC time stepping was 10^{-8}. We define Γ as the curve smoothly interpolated from 11 points in the xy-plane:
$v_1 = (4, 0.1)$, $v_2 = (4, 0.2)$, $v_3 = (4, 0.3)$, $v_4 = (4, 0.4)$, $v_5 = (2.3196, 2.3883)$,
$v_6 = (-0.26237, 2.0646)$, $v_7 = (-2.4999, 1.5231)$, $v_8 = (-3.8547, -1.4071)$,
$v_9 = (-1.1845, -3.5318)$, $v_{10} = (1.2217, -1.8909)$, $v_{11} = (4, -0.33238)$.
Tangential and normal directions can be defined for each point of Γ. The myelin layer is defined by going from Γ along the inward and outward normal directions a distance of $\eta/2$ (see Fig. 3).

The diffusion in the axons and the extra-cellular space is supposed to be isotropic. The same intrinsic diffusion coefficient $\sigma_i = \sigma_e = 3{\cdot}10^{-3}\mathrm{mm}^2/\mathrm{s}$ is set for both compartments. Diffusion inside the layer is anisotropic with the tangential diffusion coefficient $\sigma_m^\tau = 3 \cdot 10^{-3}\mathrm{mm}^2/\mathrm{s}$ and transverse diffusion coefficient σ_m^n. We simulated different permeabilities κ_0 and varied the thickness η for each permeability. The transverse diffusion coefficient σ_m^n is then computed from κ_0 and η by Eq. (3.4).

The diffusion-encoding sequence is PGSE (see Eq. (2.2)), the gradient direction is $\dfrac{\mathbf{q}}{\|\mathbf{q}\|} = \dfrac{[1,1]}{\sqrt{2}}$. The uniform distribution of water protons is used for the initial condition:

$$M(\mathbf{x}, 0) = 1. \tag{4.1}$$

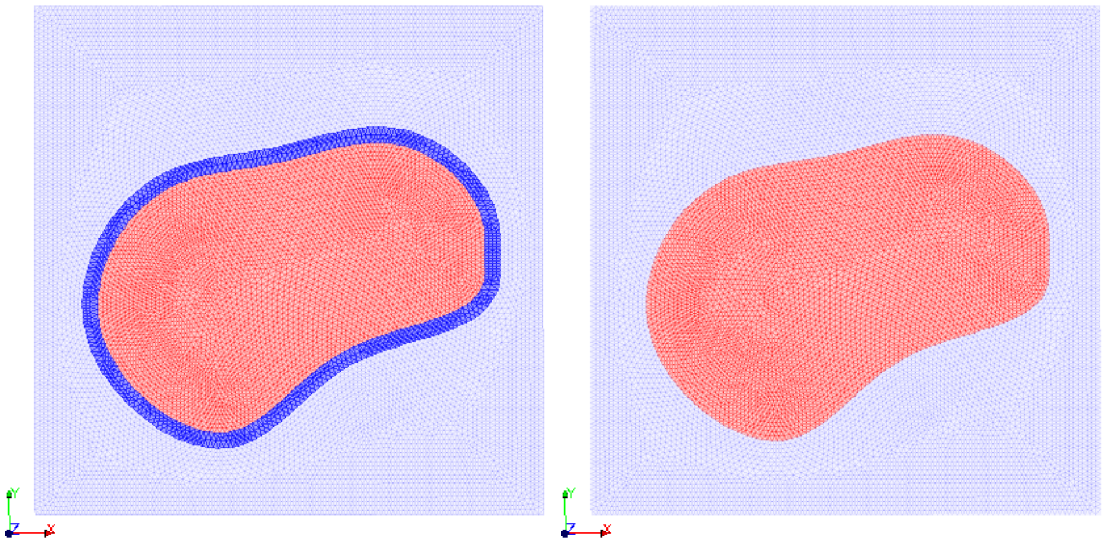

(a) (b)

Figure 3: The three-compartment model (left) and the corresponding two-compartment model (right) for an irregular shaped axon.

Reflecting boundary conditions are applied for the exterior boundaries of the computational domain C:

$$\overline{\boldsymbol{\sigma}}\nabla M \cdot \mathbf{n} = 0 \text{ on } \partial C. \tag{4.2}$$

First, we fix $\delta = \Delta = 10$ms and $b = 15000$ s/mm^2 ($\|\mathbf{q}\| \approx 4.74\,\text{mm}^{-1}\,\text{s}^{-1}$), and simulated $\kappa_0 = 10^{-5}$m/s (Fig. 4a) and $\kappa_0 = 10^{-6}$m/s (Fig. 4b). As expected, the signal of the two-compartment model with the ADTC converges quadratically to that of the corresponding three-compartment model whereas the two-compartment model with the IDTC only has first order convergence. Similarly, at $\delta = \Delta = 2$ms, $\kappa_0 = 10^{-5}$m/s, we simulated two $b-$values, 1000 s/mm^2 (Fig. 4c) and 2000 s/mm^2 (Fig. 4d), and we can see that quadratic convergence is obtained using ADTC whereas the convergence is first order for IDTC.

5. Conclusions. In this paper, we derived and validated a new transmission condition that accounts for anisotropic diffusion in thin layers. We showed numerically that this condition is second order accurate in the layer thickness, whereas a more classical transmission condition is only first order accurate. We illustrated these transmission conditions in application to diffusion MRI where the diffusion inside the myelin sheath surrounding axons is smaller in the normal direction than the tangential direction.

The anisotropic diffusion transmission condition that we propose here serve two purposes. From a numerical point of view, this approach simplifies the numerical solution of the dMRI signal model by removing the need to discretize the myelin sheath, a computational saving that may be significant in three dimensions when simulating arbitrarily oriented white matter fibers. Just as importantly, we hope that this reduction of the geometrical complexity of the model will aide in formulating a homogenized (macroscopic) model of the dMRI signal for white matter in the future (as in [9]). This will be the subject of future investigation.

REFERENCES

[1] Y. Achdou, O. Pironneau, and F. Valentin. Effective boundary conditions for laminar flows over periodic rough boundaries. *J. Comput. Phys.*, 147(1):187–218, 1998.

[2] B. Aslanyürek, H. Haddar, and H. Şahintürk. Generalized impedance boundary conditions for thin dielectric coatings with variable thickness. *Wave Motion*, 48(7):681–700, 2011.

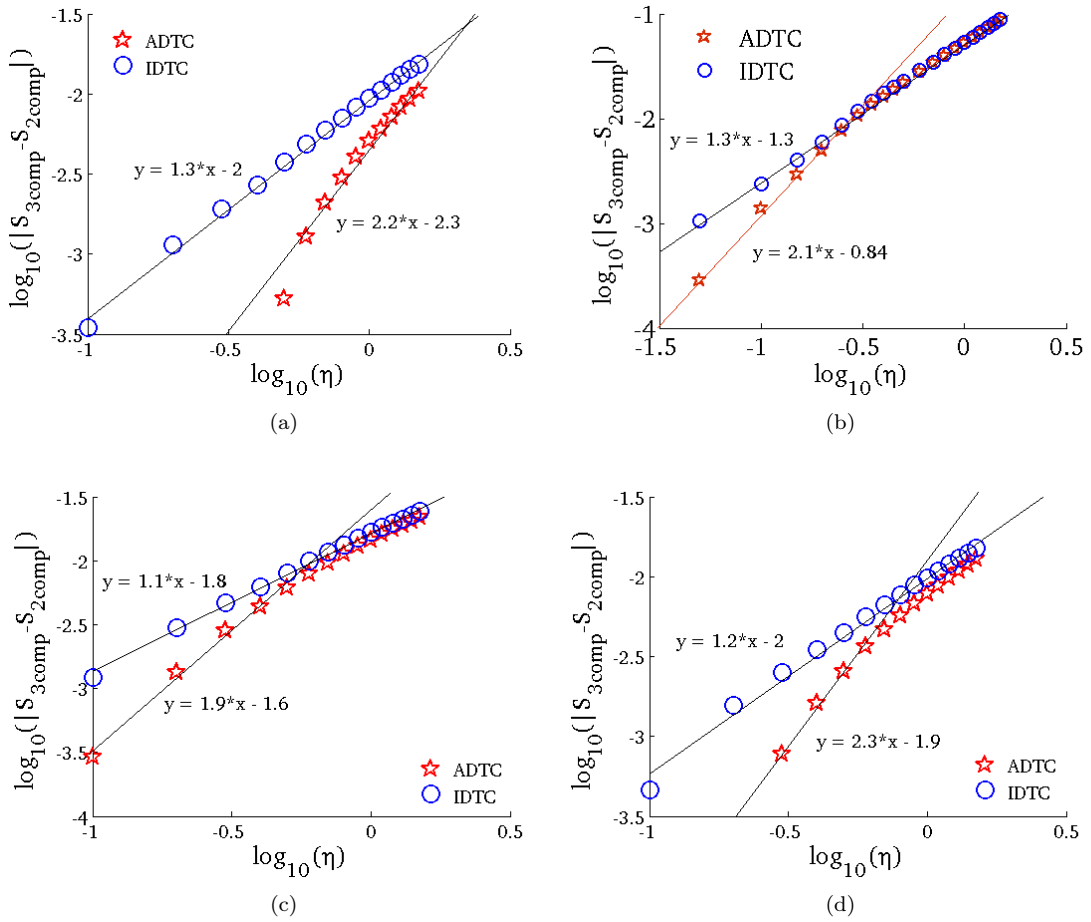

Figure 4: The signal of the new two compartment model with ADTC quadradically converges to that of the corresponding three-compartment model whereas the two compartment model with IDTC only gives the first order convergence. This result is shown at $\delta = \Delta = 10$ms and $b = 15000$ s/mm^2 ($\|\mathbf{q}\| \approx 4.74\,\mathrm{mm}^{-1}\,\mathrm{s}^{-1}$), for two different permeabilities $\kappa_0 = 10^{-5}$m/s (Fig. 4a) and $\kappa_0 = 10^{-6}$m/s (Fig. 4b). For $\delta = \Delta = 2$ms, $\kappa_0 = 10^{-5}$m/s, the quadratic convergence using ADTC and first order convergence using IDTC are shown for two $b-$values, 1000 s/mm^2 (Fig. 4c) and 2000 s/mm^2 (Fig. 4d).

[3] Y. Assaf, R. Z. Freidlin, G. K. Rohde, and P. J. Basser. New modeling and experimental framework to characterize hindered and restricted water diffusion in brain white matter. *Magnetic Resonance in Medicine*, 52(5):965–978, 2004.

[4] W. Y. Aung, S. Mar, and T. L. Benzinger. Diffusion tensor MRI as a biomarker in axonal and myelin damage. *Imaging in Medicine*, 5(5):427–440, Oct. 2013.

[5] C. Beaulieu. The basis of anisotropic water diffusion in the nervous system – a technical review. *NMR in Biomedicine*, 15(7-8):435–455, 2002.

[6] A. Bendali and K. Lemrabet. The effect of a thin coating on the scattering of a time-harmonic wave for the Helmholtz equation. *SIAM J. Appl. Math.*, 56(6):1664–1693, 1996.

[7] I. E. Biton, I. D. Duncan, and Y. Cohen. High b-value q-space diffusion MRI in myelin-deficient rat spinal cords. *Magn Reson Imaging*, 24(2):161–166, Feb. 2006.

[8] S. Chun, H. Haddar, and J. S. Hesthaven. High-order accurate thin layer approximations for time-domain electromagnetics, Part II: transmission layers. *J. Comput. Appl. Math.*, 234(8):2587–2608, 2010.

[9] J. Coatléven, H. Haddar, and J. Li. A macroscopic model including membrane exchange for diffusion MRI. *SIAM Journal on Applied Mathematics*, 74(2):516–546, 2014.

[10] B. Delourme, H. Haddar, and P. Joly. Approximate models for wave propagation across thin periodic interfaces. *J. Math. Pures Appl. (9)*, 98(1):28–71, 2012.

[11] J. Farrell. *Q-space Diffusion Imaging of Axon and Myelin Damage in the Human and Rat Spinal Cord*. Johns Hopkins University, 2009.

[12] R. Fox, T. Cronin, J. Lin, X. Wang, K. Sakaie, D. Ontaneda, S. Mahmoud, M. Lowe, and M. Phillips. Measuring myelin repair and axonal loss with diffusion tensor imaging. *American Journal of Neuroradiology*, 32(1):85–91, Jan. 2011.

[13] H. Haddar and P. Joly. Effective boundary conditions for thin ferromagnetic coatings. Asymptotic analysis of the 1D model. *Asymptot. Anal.*, 27(2):127–160, 2001.

[14] H. Haddar and P. Joly. Stability of thin layer approximation of electromagnetic waves scattering by linear and nonlinear coatings. *Journal of Computational and Applied Mathematics*, 143(2):201 – 236, 2002.

[15] H. Haddar, P. Joly, and H.-M. Nguyen. Generalized impedance boundary conditions for scattering by strongly absorbing obstacles: the scalar case. *Math. Models Methods Appl. Sci.*, 15(8):1273–1300, 2005.

[16] H. Haddar, P. Joly, and H.-M. Nguyen. Generalized impedance boundary conditions for scattering problems from strongly absorbing obstacles: The case of Maxwell's equations. *Mathematical Models and Methods in Applied Sciences*, 18(10):1787–1827, 2008.

[17] M. A. Horsfield and D. K. Jones. Applications of diffusion-weighted and diffusion tensor MRI to white matter diseases, a review. *NMR Biomed.*, 15(7-8):570–577, 2002.

[18] W. Jäger and A. Mikelić. On the roughness-induced effective boundary conditions for an incompressible viscous flow. *J. Differential Equations*, 170(1):96–122, 2001.

[19] H. Johansen-Berg and T. Behrens. *Diffusion MRI: From quantitative measurement to in vivo neuroanatomy.* Elsevier Science, 2013.

[20] D. Jones. *Diffusion MRI: theory, methods, and applications.* Oxford University Press, USA, 2010.

[21] L. J. Lanyon. *Neuroimaging - Methods*, chapter Diffusion tensor imaging: structural connectivity insights, limitations and future directions, page DOI: 10.5772/23245. InTech, 2012.

[22] D. Le Bihan and H. Johansen-Berg. Diffusion MRI at 25: Exploring brain tissue structure and function. *NeuroImage*, 61(2):324–341, June 2012.

[23] D. LeBihan. The 'wet mind': water and functional neuroimaging. *Physics in medicine and biology*, 52(7):–, Apr. 2007.

[24] J.-L. Lions. Quelques remarques sur les équations différentielles opérationnelles du $\mathbf{1^{er}}$ ordre. *Rend. Sem. Mat. Univ. Padova*, 33:213–225, 1963.

[25] J.-L. Lions and E. Magenes. *Non-homogeneous boundary value problems and applications. Vol. I.* Springer-Verlag, New York-Heidelberg, 1972. Translated from the French by P. Kenneth, Die Grundlehren der mathematischen Wissenschaften, Band 181.

[26] S. E. Maier, Y. Sun, and R. V. Mulkern. Diffusion imaging of brain tumors. *NMR Biomed.*, 23(7):849–864, 2010.

[27] D. V. Nguyen, J.-R. Li, D. Grebenkov, and D. L. Bihan. A finite elements method to solve the Bloch-Torrey equation applied to diffusion magnetic resonance imaging. *Journal of Computational Physics*, 263(0):283 – 302, 2014.

[28] C. Poignard. Generalized impedance boundary condition at high frequency for a domain with thin layer: the circular case. *Applicable Analysis*, 86(12):1549–1568, 2007.

[29] R. Quarles, W. Macklin, and P. Morell. *Basic neurochemistry: molecular, cellular and medical aspects*, chapter Myelin formation, structure and biochemistry. Elsevier Science, 2006.

[30] B. P. Sommeijer, L. F. Shampine, and J. G. Verwer. RKC: an explicit solver for parabolic PDEs. *J. Comput. Appl. Math.*, 88(2):315–326, 1998.

[31] E. O. Stejskal and J. E. Tanner. Spin diffusion measurements: Spin echoes in the presence of a time-dependent field gradient. *The Journal of Chemical Physics*, 42(1):288–292, 1965.

[32] H. Torrey. Bloch equations with diffusion terms. *Physical Review Online Archive (Prola)*, 104(3):563–565, 1956.

[33] J. G. Verwer, W. H. Hundsdorfer, and B. P. Sommeijer. Convergence properties of the Runge-Kutta-Chebyshev method. *Numer. Math.*, 57(2):157–178, 1990.